JMEPEG (1993) 2:659-664

Hot-Pressing of TiC-Graphite Composite Materials

T. Ono, H. Endo, and M. Ueki

Monolithic TiC and TiC-graphite composites were hot-pressed at temperatures ranging from 1800 to 2100 °C and with graphite contents up to 30 wt%. Densification behavior was compared for both monolith and composites based on results of microstructural observation and mechanical tests. Monolithic TiC was well densified at the hot-pressing temperature of 1800 °C; significant grain growth and an accompanying decrease in the flexural strength occurred with an increase in hot-pressing temperature. Conversely, the 10 wt% graphite-containing TiC composite required higher temperatures (1900 to ~2000 °C) to reach a similar degree of densification approaching that of monolithic TiC. As with densification, flexural strength of the composite increased with an increase in hot-pressing temperature. Graphite dispersions in the composites inhibited grain growth of TiC. Contrary to the equiaxed nature of the monolithic TiC grains, in the composite system, the graphite grains were flattened to thin platelets that aligned perpendicular to the hot-pressing axis. Apparent anisotropy in the microstructure was observed in the composites. At a fixed hot-pressing temperature, the relative density of the composites decreased with increasing graphite content.

Keywords

densification, graphite, hot-pressing, mechanical properties, microstructure, TiC

1. Introduction

TITANIUM carbide (TiC) is a covalently bonded ceramic material characterized by high hardness, a high melting point, and high strength. Additionally, TiC exhibits similar electrical conductivity to metallic materials. TiC powder, with its fine size, exhibits relatively good sinterability. In spite of such attractive characteristics, application of TiC has been limited because of its inherent brittleness[1] at room temperature. Dispersoids in cermets and ceramic matrix composites or thin (and thick) films for coating use are the only examples of those limited applications of TiC. To increase the application of TiC in structural use, addition of a secondary phase to form a composite can be effective. Endo et al.[2,3] investigated TiC-SiC ceramic composites, focusing on the mechanical and electrical properties of the composites, and reported significant improvement in flexural strength and fracture toughness due to the formation of a duplex microstructure.

In addition to such TiC-based ceramic composites, the authors have focused on graphite as the secondary phase in the TiC matrix. Although graphite has a much lower strength compared to TiC, when added to the TiC, it is expected to reduce the oxide layer on the surface of TiC particles, lower the specific gravity of the composite, provide self-lubricant action in sliding parts, and improve mechanical properties. Using carbon black as the carbon source, Ueno et al.[4] fabricated 1 wt% B_4C-doped TiC/carbon composites with a carbon content of 15 wt% or less by hot-pressing. They reported that there was some evidence of graphitization of the carbon black and some improvement in strength and toughness by the addition of carbon.

T. Ono, H. Endo, and **M. Ueki,** Advanced Materials & Technology Research Laboratories, Nippon Steel Corporation, Nakahara-ku, Kawasaki, Japan.

In the present work, the effect of hot-pressing temperature on densification and mechanical properties of 10 wt% graphite-containing TiC composites compared to monolithic TiC was investigated in connection with microstructural analysis. Mechanical properties of a series of TiC-0 to ~30 wt% graphite composites hot-pressed under fixed conditions were studied, focusing on the correlation between graphite content and microstructure.

2. Experimental

2.1 *Fabrication of TiC-Graphite Composites*

TiC powder, with an average particle size of 2 μm and purity of >99% (Kojundo Kagaku Co., Ltd., Saitama, Japan), and well graphitized (interlayer distance = 0.3357 nm) carbon platelets, with an average size of about 4 μm in diameter and 1 μm or less in thickness (Lonza Ltd., Sins, Switzerland), were mixed in 0.2 vol% polyoxyethylene sorbitan monolaurate (surfactant) water solution for 17 h by planetary ball mill. The slurry was dehydrated by suction and dried for 24 h in an oven at 110 °C. The dried powder mixture was crushed with a mortar. Powder processing was omitted for monolithic TiC. The prepared powder was hot-pressed in a 90 × 60 mm graphite die. In the first experimental series, the hot-pressing (HP) temperatures ranged from 1800 to ~2100 °C to determine the effects of temperature on the microstructure and mechanical properties of monolithic TiC and 10 wt% graphite-containing TiC composites. In another series of experiments, the HP temperature was maintained at 2000 °C to investigate the effect of graphite content on the characteristics of a series of TiC-0 to ~30 wt% graphite composites. Holding time of 120 min and applied pressure of 40 MPa were chosen for the HP operation in both series of experiments. A flowchart of the experimental procedure from powder processing to the evaluation of hot-pressed bodies and heat and pressure patterns adopted in the hot-pressing operations are shown in Fig. 1. The six types of TiC-graphite composites that were fabricated and tested are listed in Table 1.

Table 1 TiC-graphite composites and graphite contents

	Graphite content					
wt%	5	10	15	20	25	30
vol%	10.4	19.6	27.9	35.4	42.3	48.5

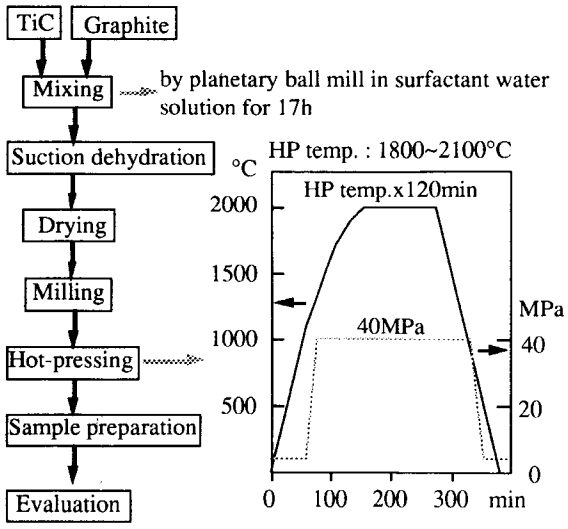

Fig. 1 Flowchart of the experimental procedure from powder processing to evaluation of hot-pressed bodies and the heat and pressure schedule for the hot-pressing operation.

2.2 *Microstructural Analysis*

Microstructural features were characterized by observation of polished surfaces using both optical and scanning electron microscopy (SEM). Some of the samples were etched in a solution composed of an equal mixture of nitric acid (60% conc) and hydrofluoric acid (46% conc) for 60 to 1800 s. Average grain diameter was measured from mean intercept length using the stereology[5] method, where the average grain diameter was determined by the product of a constant depending on the shape of the grain and the average code length by multiple linear measurements on the micrographs. Fracture surfaces after flexural tests were also observed by SEM.

2.3 *Evaluation of Mechanical Properties*

Bulk density was measured by the Archimedes method, and relative density was calculated by using 4.94 g/cm^3 for the theoretical density (TD) of TiC and 2.26 g/cm^3 for that of graphite. Flexural strength at room temperature was measured by three-point bending tests with a span length of 30 mm and a cross head speed of 0.05 mm/min (JIS R1601). Fracture toughness was evaluated using the technique specified by JIS R1607 (SEPB method). Hardness was measured by JIS Z2244 (Vickers hardness) with an indentation load of 98 N and a holding time of 10 s. To determine the difference in mechanical properties due to the microstructural anisotropy originating from the difference in HP direction, two different methods were adopted to machine the test samples from hot-pressed plate, as shown in Fig. 2.

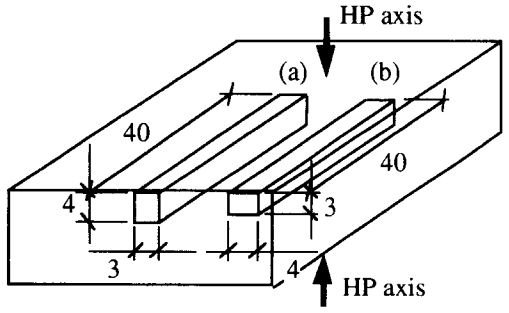

Fig. 2 Schematic configuration of sampling flexural bars from the hot-pressed plate (60 × 90 × 13 mm); (a) loading direction normal and (b) parallel to the HP axis.

3. Results and Discussion

3.1 *Densification by hot-pressing*

Relative density, room temperature flexural strength, and average TiC grain diameter for monolithic TiC and 10 wt% graphite-containing TiC composite as a function of HP temperature are shown in Fig. 3. In Fig. 3(a), densification of around 98% TD was achieved in monolithic TiC over the entire range of the temperatures tested. The density of the 10 wt% graphite-containing TiC composite increased from 91.5 % TD at 1800 °C to 97% TD at 1900 °C, becoming almost constant up to 2100 °C. A significant difference in sinterability between monolithic and 10 wt% graphite-containing TiC was apparent. The flexural strength of the composite increased with HP temperature, as shown in Fig. 3(b); that of monolithic TiC, on the other hand, decreased with the increase in temperature. Figure 3(c) illustrates the HP temperature dependence of the average grain diameter of the sintered bodies measured from the optical micrographs of monolithic TiC and the TiC-graphite composite using the technique described previously. The average grain diameter was much larger in monolithic TiC compared to the composite and increased with HP temperature. The degree of grain growth was also higher in monolithic TiC. Optical micrographs taken from the etched surfaces of monolithic TiC hot-pressed at 1800 and 2100 °C are shown in Fig. 4(a) and (b), respectively. The grain diameter increased from 7 to 28 μm with an increase in temperature. The dark areas in the micrographs are thought to be mainly intrinsic pores or defects brought about by grinding and polishing. According to high-resolution SEM studies, some were found to be impurities primarily consisting of carbon. The most likely source is free carbon in the TiC raw powder. Grain shape is rather equiaxed, and anisotropy in the microstructure caused by differences in areas parallel or perpendicular to the HP direction was not observed.

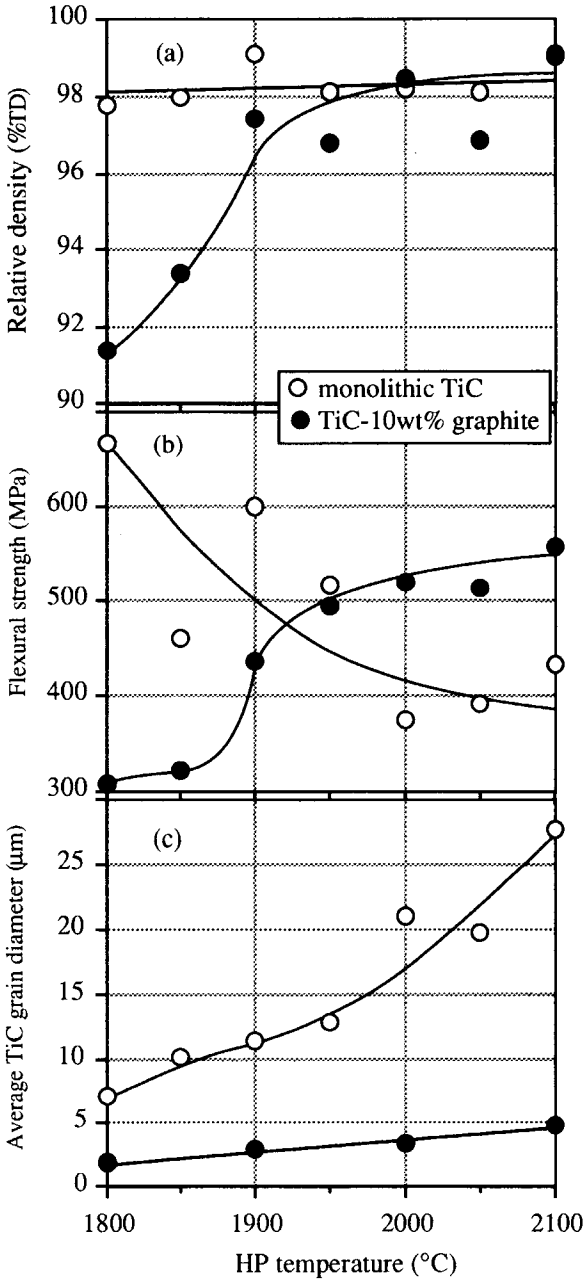

Fig. 3 Hot-pressing temperature dependence of (a) the relative density, (b) flexural strength, and (c) average TiC grain diameter for monolithic and 10 wt% graphite-containing TiC.

Figure 5 shows the optical micrographs of 10 wt% graphite-containing TiC composite hot-pressed at 2100 °C, where dark and light gray areas in the micrographs correspond to dispersed graphite and TiC, respectively. Contrary to the monolithic TiC, the TiC grains are inhibited from coalescing each other by the dispersed graphite phase. In the area parallel to the HP axis, graphite tends to lie horizontally in the micrograph (Fig. 5a), whereas in areas perpendicular to the axis, the graphite clusters or dark areas are distributed randomly and are equiaxed in shape (Fig. 5b). High-resolution SEM fractographs are shown

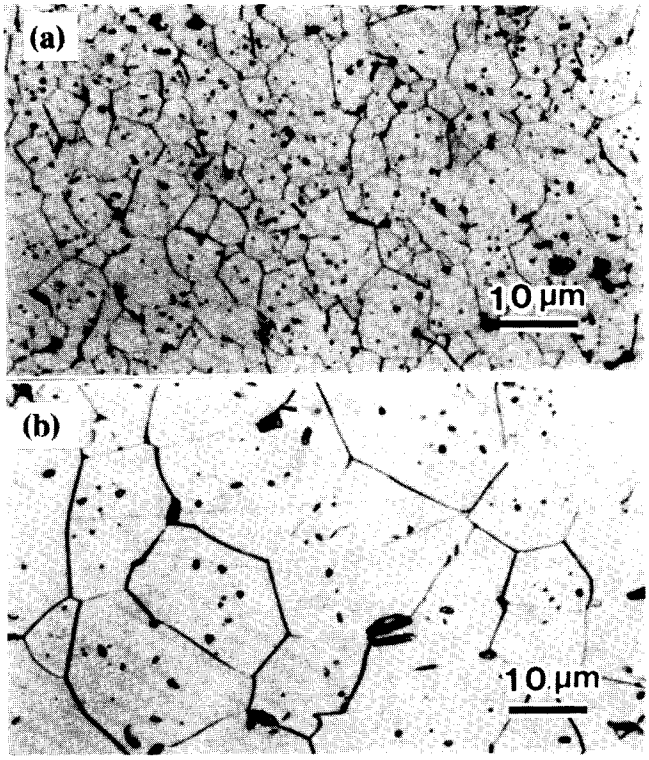

Fig. 4 Optical micrographs of etched surface of monolithic TiC hot-pressed at (a) 1800 °C and (b) 2100 °C.

in Fig. 6(a) and (b) for monolithic TiC (hot-pressed at 2000 °C) and the TiC-10wt% graphite composite (hot-pressed at 2100 °C), respectively. The fracture mode of monolithic TiC was primarily transgranular, whereas the composites fractured intergranularly when cracks propagated parallel to the longitudinal direction of graphite clusters. Propagation of both cracks was normal and parallel to the graphite clusters, as shown in Fig. 7(a) and (b). Apparently, significant crack deflection occurred for the configuration shown in Fig. 7(a), and straightforward propagation was observed in Fig. 7(b). Both an increase and decrease in the strength for the composite and monolith TiC with an increase in HP temperature occurred via densification and secondary phase incorporation. In the case of monolithic TiC, the loss of strength with a constant level of densification is apparently due to grain growth, as shown in Fig. 4. Generally, in metallic materials, strength, σ, decreases with an increase in the grain size, d, following the Hall-Petch[6] relation, $\sigma \propto d^{-1/2}$. Similar to the results obtained in previous work on high-purity alumina,[7] the grain size dependence of strength in monolithic TiC can be correlated by this relation, as shown in Fig. 8. As an additional cause for the loss of strength in materials hot-pressed at the higher temperatures, coalescence of inclusions, which consists mainly of free carbon contained in the TiC raw powder as the impurity component, must be considered. At higher temperatures, the intensive coalescence of TiC grains, accompanied with increased mobility of the inclusion, facilitated growth of the inclusion at a triple point of the grain boundaries. A coalescent inclusion tends to act as the fracture origin when its size exceeds a certain critical value.

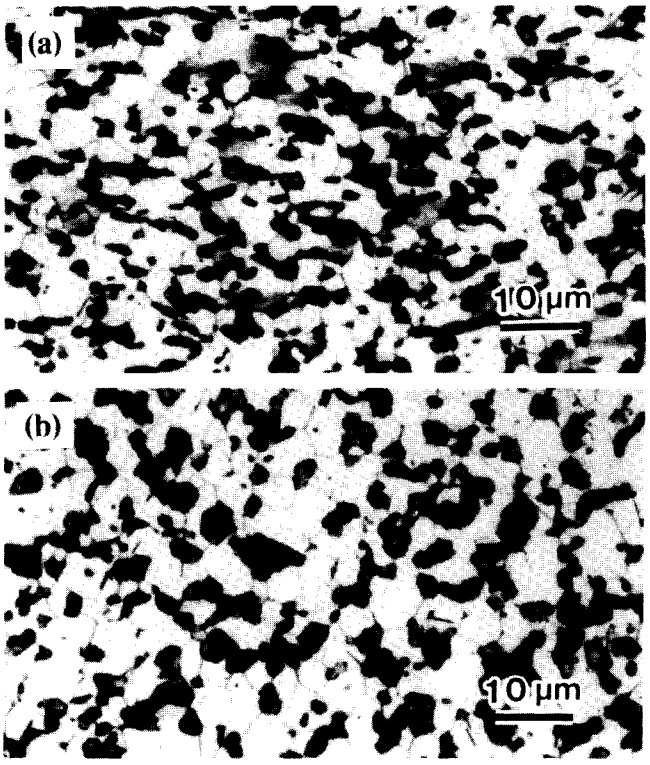

Fig. 5 Optical micrographs of 10 wt% graphite-containing TiC on the section parallel (a) and perpendicular (b) to the hot-pressing axis.

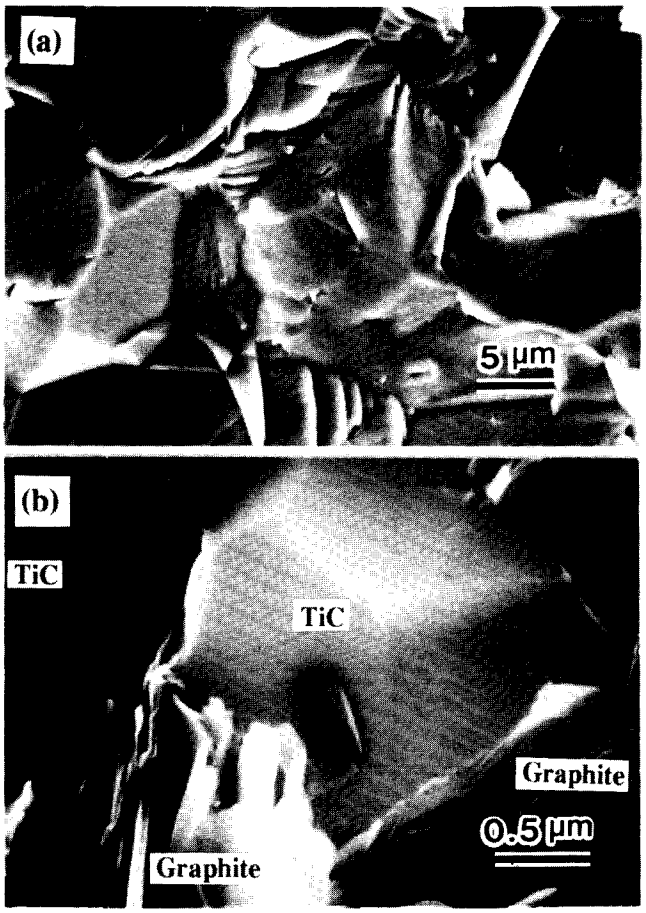

Fig. 6 SEM fractographs of (a) monolithic TiC hot-pressed at 2000 °C and (b) 10 wt% graphite-containing TiC hot-pressed at 2100 °C.

On the other hand, mechanical properties of the composite improved with increased densification due to increasing HP temperature. In the relationship between flexural strength and HP temperature, as shown in Fig. 3(b), both curves for monolithic TiC and the composite crossed between 1900 and 2000 °C. This range of temperature coincides with that at which the degree of densification for both materials becomes almost the same (see Fig. 3a). Namely, for an HP temperature higher than 1950 °C, the TiC-10 wt% graphite composite exhibited higher flexural strength than monolithic TiC by inhibiting the TiC grain growth through the incorporation of platelet graphite clusters adjacent to the TiC grains. In many cases, the graphite clusters between the TiC grains acted as a direct barrier to grain growth through coalescence. Then, TiC grain growth was minimized in the composite hot-pressed even at 2100 °C to 5 μm or less in size compared to 7 μm for monolithic TiC hot-pressed at 1800 °C.

3.2 *Effect of Graphite Content on the Mechanical Properties*

In a series of TiC-0 to ~30 wt% graphite composites, hot-pressed at 2000 °C and held for 2 h at a pressure of 40 MPa, mechanical properties were evaluated. Bulk and relative densities of the composites as a function of graphite content (wt%) are shown in Fig. 9(a). At the HP condition, relative density increased up to 5 wt% graphite addition and subsequently decreased with further graphite additions. The reasons for the increase in relative density due to the 5 wt% graphite addition may be explained as follows. First, some of the graphite incorporated into the TiC matrix was consumed to reduce the oxide layer on the surface of TiC particles during hot-pressing, which increases the bulk density substantially. Second, in the case of small graphite additions, because graphite particles are barely in contact with each other, their poor sinterability does not affect densification of the TiC matrix. However, the larger the graphite addition, more frequent graphite-graphite contact occurs. In composites with higher graphite content, the poor sinterability of graphite affects densification.

Figure 9(b) illustrates the flexural strength versus graphite content relationship, where two types of specimens were prepared by the method described in Fig. 2. The difference between the two specimens was negligible, and the flexural strength reached a maximum at 5 wt% graphite addition for both specimens. The maximum strength achieved at 5 wt% graphite addition can be attributed to the inhibition of grain growth in the TiC grains, as discussed in the former section. A decrease in strength with further additions may result from both decreasing of relative density and the addition of weaker material (graphite).

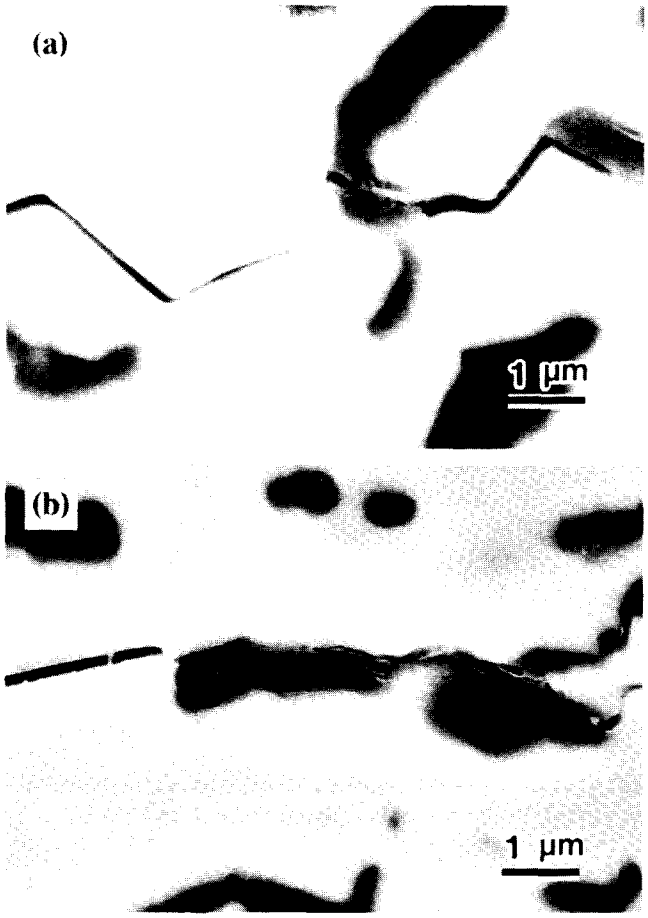

Fig. 7 Crack propagations from Vickers indentations on surfaces parallel (a) and perpendicular (b) to the HP axis of 10 wt% graphite-containing TiC composite.

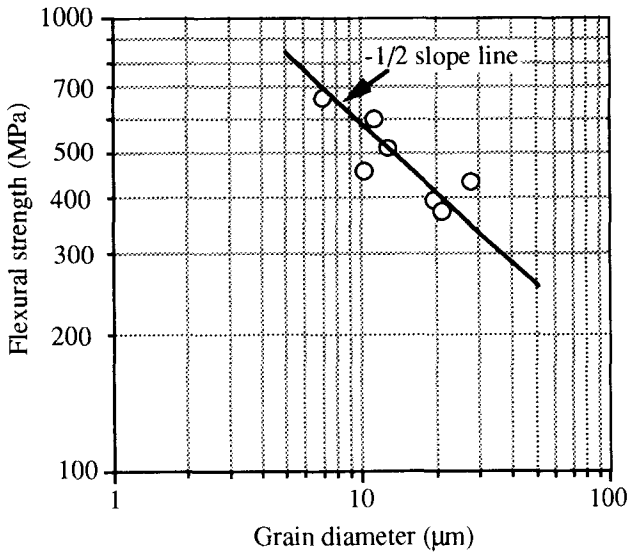

Fig. 8 Grain size dependence of flexural strength in monolithic TiC.

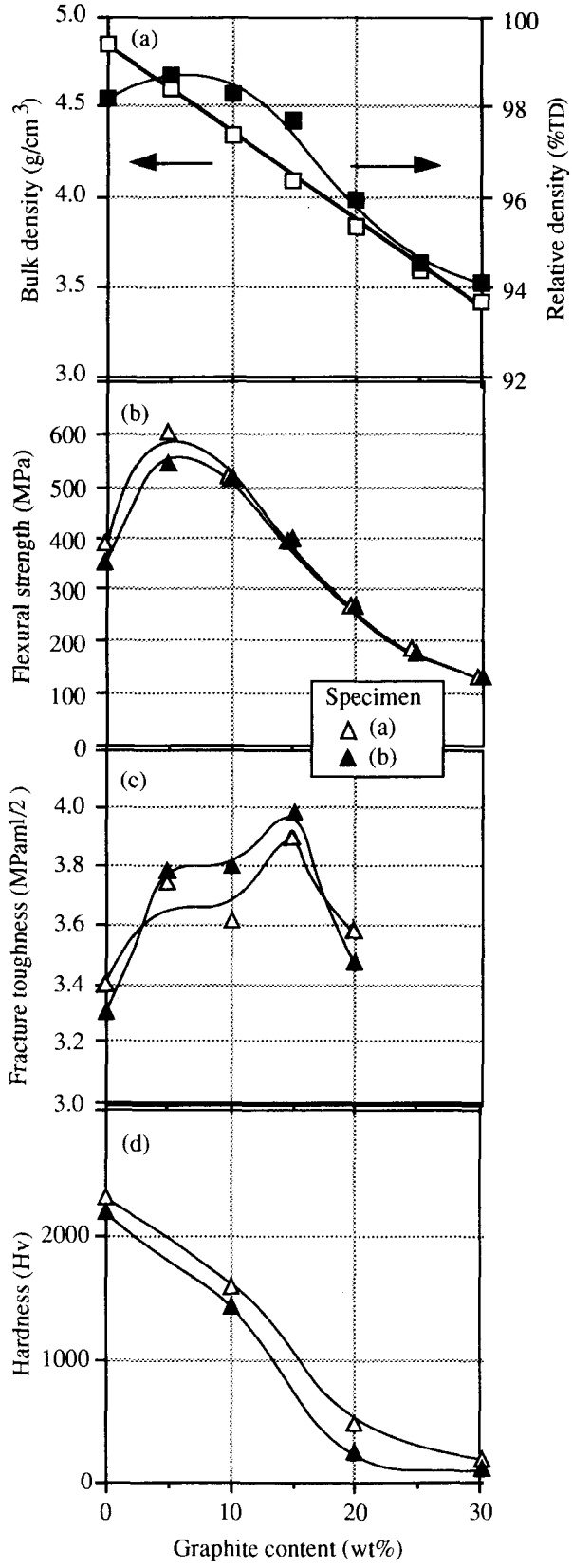

Fig. 9 Properties of a TiC-graphite composite hot-pressed at 2000 °C as a function of graphite content; *n* and *p* correspond to Fig. 2.

Fracture toughness as a function of graphite content is shown in Fig. 9(c). An increase of about 20% in fracture toughness from monolithic TiC was reported with the 15 wt% graphite addition. Toughening may be attained by crack deflection, as shown in Fig. 7. In the TiC-graphite composite, the crack was deflected by dispersed graphite, due to the presence of residual stress developed by the difference in the thermal expansion coefficient and elastic modulus between the matrix and the secondary phase.

As shown in Fig. 9(d), the Vickers hardness of the composites decreased significantly with an addition of graphite. Different from strength and toughness, hardness exhibited a certain difference between the two types of the specimens, which may be related to the orientation of graphite layers. In the case of indentation on the plane parallel to the HP axis, in which graphite platelets tend to stack on the plane, the indentation force seems to be absorbed by an apparent deformation of the graphite phase. On the other hand, in the case of indentation perpendicular to the HP axis, in which the graphite layers tend to lie normal to the plane, fewer graphite platelets can absorb the indentation force. The composites, therefore, exhibit smaller deformation, that is, higher hardness.

4. Conclusions

Hot-pressing of monolithic TiC and TiC-graphite composites was investigated, focusing on densification, microstructure, and mechanical properties of the sintered bodies. Experimental variables included HP temperature, ranging from 1800 to 2100 °C, and graphite content up to 30 wt%. Results obtained can be summarized as follows.

Monolithic TiC was well densified by hot-pressing at 1800 °C, and significant grain growth occurred with an accompanying decrease in the flexural strength at higher hot-pressing temperature. The 10 wt% graphite-containing TiC composite required a higher temperature for hot-pressing to densify to the same extent as the monolithic TiC due to the poor sinterability of graphite. The flexural strength of the composite increased with an increase in hot-pressing temperature.

Graphite platelets lying on the boundaries of the TiC grains inhibited the growth of TiC grains. Although microstructural anisotropy was not observed in monolithic TiC, TiC-graphite composites exhibited anisotropy in that the planes of the graphite platelets were perpendicular to the HP axis.

Under fixed hot-pressing conditions, the relative density of the TiC-graphite composite decreased with an increase in graphite content, whereas the 5 wt% graphite addition exhibited a maximum in flexural strength and 20% increase in fracture toughness. The 15 wt% graphite addition attributed to crack deflection due to the secondary phase incorporation.

References

1. D.K. Chatterjee, M.G. Mendiratta, and H.A. Lipsitt, *J. Mater. Sci.*, Vol 14, 1979, p 2151-2156
2. H. Endo, M. Ueki, and H. Kubo, *J. Mater. Sci.*, Vol 25, 1990, p 2103-2506
3. H. Endo, M. Ueki, and H. Kubo, *J. Mater. Sci.*, Vol 26, 1991, p 3769-3775
4. K. Ueno, S. Sodeoka, and M. Yano, *J. Ceram. Soc. Jpn.*, Vol 97, 1989, p 507-512
5. E.E. Underwood, A.R. Colcord, and R.C. Waugh, *Ceramic Microstructures*, R.M. Fulrath and J.A. Pask, Ed., Robert E. Kringer Publishing, 1966, p 25-52
6. C.R. Barrett, W.D. Nix, and A.S. Tetelman, *The Principles of Engineering Materials*, Prentice-Hall, 1973, p 267
7. M. Ueki and H. Endo, unpublished work